

Using a Digital Camera for Colorimetry of Human Teeth

Wencheng Wu and Jan P. Allebach

School of ECE, Purdue University, West Lafayette, Indiana

Mostafa Analoui

School of Dentistry, Indiana University, Indianapolis, Indiana

Abstract

Accurate assessment of the color of human teeth is important for the specification of color for dental restorations, as well as the evaluation of the efficacy of treatment processes that are intended to restore natural tooth color. We are investigating the use of a Kodak model DCS460c digital camera for colorimetry of teeth. Our objective is to obtain CIE XYZ tristimulus coordinates from the raw rgb data acquired by the camera. Our model consists of a set of 3 nonlinearities for gray balance, followed by a 3×3 matrix transformation. Using this model, we have achieved an average error of 1.4507 ΔE units over a set of 180 color samples, 0.9703 ΔE units over a Bioform shade guide, and 1.5745 ΔE units over a set of 11 extracted human teeth.

Introduction

Conventionally, dentists determine the color of human teeth via visual comparison to a standard set called a shade guide. This process requires technical training and artistic judgment. When the color of the tooth does not match one of the samples in the shade guide, the technician will adjust the Munsell coordinates of the nearest shade guide sample based on the visual difference between that sample and the tooth. Even though many researchers have suggested systematic approaches to shade selection,¹⁻⁴ matching based on visual comparison remains a very inefficient approach; and subjective human errors are a significant problem.

Furthermore, it has been shown that several existing shade guides are inadequate to represent the color space of human teeth.^{4,6} An additional source of difficulty is the fact that shade guides are constructed from materials that are different from those used for the restoration,⁴ e.g. bridge or crown, etc. This limits the accuracy of using a shade guide as a standard to specify the color for the restoration. All of these errors may be reduced with proper training, accumulated experience, and development of better shade guides. The effectiveness of the shade guide is impacted by both the choice of colors for the samples, which is typically based on the colors of natural teeth, and the arrangement

of the samples in the guide. A number of solutions to this problem have been proposed.⁷⁻⁹

Even if all the preceding difficulties can be resolved, we must still deal with metamerism. The illumination condition in most clinical offices may match the work environment of the patient; but it is nothing like that to which the patient is exposed in other parts of his or her daily life, such as daylight, cozy dim light in the living-room, etc. A match in the clinical office does not guarantee a match under another illuminant. It is important to obtain a good match under all conditions of illumination; and this cannot be achieved by methods based on visual comparison.

An alternative is to use a traditional spectroradiometer or spectrophotometer.¹⁰⁻¹³ The advantage of this approach is that the full visual range of the spectral power distribution is obtained. Nonetheless, there are several disadvantages of this measurement technique. First of all, it yields only spot measurements. Its spatial resolution is very limited. This is especially important here because with natural teeth, the color varies widely across the surface of the tooth. Secondly, the spectroradiometer is not well suited to use in the dental office setting because of the difficulty of setting up the instrument. Finally, the natural translucence of the tooth, its uneven and highly polished surface, and the effect of wetness of that surface make the measurement task even more difficult.

In this paper, we take a different route to assess the color of human teeth. We propose a method that uses a digital camera for colorimetry of human teeth. The objective of our color calibration is to provide a precise device-independent CIE XYZ tristimulus vector color descriptor for dentistry applications.

Color calibration techniques have been widely used in cross media reproduction. Several techniques have been developed for a scanner or digital camera. One common method is to use a 3×3 matrix to transform scanner/camera RGB to CIE XYZ. Wandell and Farrell^{14,15} used a training set and a least squares method to minimize ΔE . Finlayson and Drew¹⁶ utilized the information of spectral sensitivities of color devices and an assumption regarding sample reflectances to find this 3×3 calibration matrix. The major

difference between these two approaches is that the former functions well with color samples that are close to the training set, but may perform poorly when the test color is outside the training set. The latter approach performs reasonably well over a large set of colors, but is inferior within a restricted set of colors. Both methods are linear transformations; and the matrix size is restricted by the number of channels that the color device possesses.

Farrell et al¹⁷ used a color transparency to increase the number of available channels. In this case, the matrix becomes 6×3 . Kang^{18,19} proposed a two step process to map RGB to CIE XYZ: gray balancing followed by a polynomial transformation. Lenz et al²⁰ and Haneishi²¹ also proposed polynomial transformations to minimize ΔE . In general, these nonlinear methods perform better on the training set, because the linear model is a restricted version of the polynomial case. However, a high degree polynomial tends to over fit the data set. Kang and Anderson²² proposed an even more sophisticated model which uses a neural network to transform RGB to CIE XYZ.

For our purpose, we propose a simple 3-D model as depicted in Fig. 1 for the color calibration task. It consists of a set of 3 nonlinearities for gray balance followed by a 3×3 matrix transformation. Our objective is to find an optimal set of model parameters which minimizes the total least square calibration error in the CIE XYZ color space. Our model is appropriate under two situations.^{14,23} The first occurs when the camera is colorimetric. However, this is seldom true for currently available devices. The other situation occurs when the color space of interest can be well approximated by bases of three from a principal component analysis.

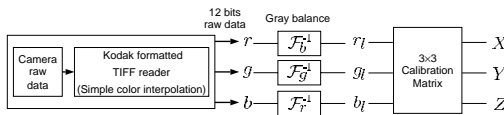


Figure 1: Simple 3-D calibration model.

Our measurement shows that 99.29% of the energy in the spectral power distribution of a set of 11 extracted teeth can be characterized by just the first three basis functions from a principal component analysis. This satisfies the requirement for a simple 3-D model.

In this paper, we present the color calibration results for our model applied to CRT generated color samples, samples from the Bioform shade guide,²⁴ and a set of extracted human teeth. In addition, we present an analysis of the effect of measurement error in the testing set on the model performance. We perform a similar analysis of the effect of measurement error in the training set. In both cases, we specifically consider the effect of quantization of data set to determine the number of bits required to achieve a given level of performance.

3-D calibration model

In this section, we describe a simple 3-D calibration model for the Kodak DCS460c digital camera. It includes a gray balance procedure followed by a 3×3 matrix. We extract 12-bit spatially multiplexed raw rgb data directly from the camera hard drive and pattern correct it according to the procedure described in Kodak Programmer's Manual.²⁵ We then interpolate to obtain full resolution channels of rgb data.

Camera nonlinearity and its gray balance

Let e denote the camera exposure time; and let $s_l(\lambda)$ and n_l denote the l th channel sensor response and its measurement noise, respectively. Let $c(\lambda)$ be the spectral power distribution of a color sample. Then the l th channel raw data acquired by the camera can be modeled as²⁶

$$l = \mathcal{F}_l \left(e \int_{\lambda} s_l(\lambda) c(\lambda) d\lambda + n_l \right) \quad l = r, g, b. \quad (1)$$

Here $\mathcal{F}_l(\cdot)$ is the camera nonlinearity of the l th channel. Suppose that the measurement noise n_l is negligible; we can determine the nonlinearity of the camera in the following two step procedure. We first fix the exposure time e and take pictures of a set of 25 gray patches. The significance of these color signals is that they have the same spectral shape and vary only within a multiplication factor; that is, they have the form of $k_m c_0(\lambda)$, where m is the index of the gray patch. Fig. 2 shows the nonlinearity of our camera at a 4 second exposure. Next, we determine our camera nonlinearity along the exposure time axis by varying e while taking pictures of a fixed gray patch. The result is shown in Fig. 3. These two curves are often referred to as gray balance curves which in effect are equivalent to the operation of $\mathcal{F}^{-1}(\cdot)$.

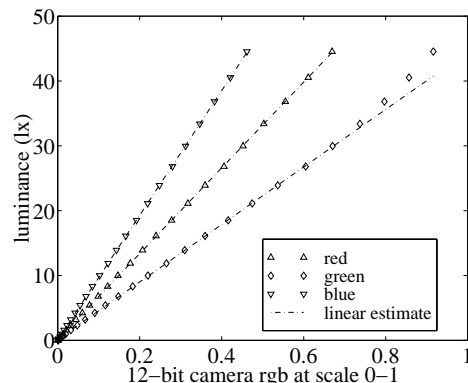


Figure 2: Camera nonlinearity at 4 second exposure. Here the 12-bit camera rgb is normalized to 0-1 scale, i.e. the unsigned 12-bit integer rgb value is divided by $(2^{12}-1)$.

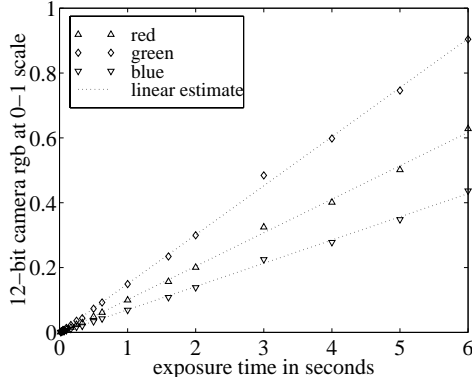


Figure 3: Camera nonlinearity across exposure time.

Parameter estimation of the 3×3 matrix

Let S be the stack of the gray-balanced camera rgb values; and let T be stack of the true tristimulus values of the color samples. Let M be the transformation from camera linear rgb values to CIE XYZ values. Our model suggests that $T \approx SM$ or more precisely speaking

$$T = SM + E, \quad (2)$$

where

$$S = \begin{bmatrix} r_1 & g_1 & b_1 \\ r_2 & g_2 & b_2 \\ \vdots & \vdots & \vdots \\ r_{N_1} & g_{N_1} & b_{N_1} \end{bmatrix},$$

$$T = \begin{bmatrix} X_1 & Y_1 & Z_1 \\ X_2 & Y_2 & Z_2 \\ \vdots & \vdots & \vdots \\ X_{N_1} & Y_{N_1} & Z_{N_1} \end{bmatrix},$$

and E is the calibration error matrix. The calibration procedure is thus formulated as a least-square problem

$$\widehat{M} = \arg \min_M \sum_{i=1}^{N_1} \|[X_i \ Y_i \ Z_i] - [r_i \ g_i \ b_i]M\|^2, \quad (3)$$

and the solution is

$$\widehat{M} = S^\dagger T = (S^t S)^{-1} S^t T. \quad (4)$$

In this paper, we refer to these N_1 color samples used for calibration model identification as the training set and the remaining samples as the testing set.

Error analysis

Let (S_1, T_1) be the stacks of the training set; and let (S_2, T_2) be the stacks of the testing set. Consider a given calibration matrix M identified by the training set (S_1, T_1) . Let $s_i = [r_i \ g_i \ b_i]$ and $t_i = [X_i \ Y_i \ Z_i]$ be the i th row of the

stacks S_2 and T_2 of the testing set. Let $u_i = [L_i^* \ a_i^* \ b_i^*]$ be the tristimulus row vector of the i th test sample in the $L^*a^*b^*$ color space, which is calculated from t_i by

$$u_i = f(t_i), \quad (5)$$

$$= \begin{bmatrix} 116\varphi\left(\frac{Y}{Y_n}\right) - 16 \\ 500\left(\varphi\left(\frac{X}{X_n}\right) - \varphi\left(\frac{Y}{Y_n}\right)\right) \\ 200\left(\varphi\left(\frac{Y}{Y_n}\right) - \varphi\left(\frac{Z}{Z_n}\right)\right) \end{bmatrix}^t, \quad (6)$$

where

$$\varphi(x) = \begin{cases} x^{1/3} & x > 0.008856 \\ 7.787x + \frac{16}{116} & x \leq 0.008856 \end{cases}.$$

Let $\Delta s_i = [\Delta r_i \ \Delta g_i \ \Delta b_i]$ be the noise in the rgb channels of the i th test sample. Then from Eq. (2), the variation of tristimulus values Δt_i is

$$\Delta t_i = ((s_i + \Delta s_i)M) - s_i M = \Delta s_i M. \quad (7)$$

Accordingly, the variation Δu_i is

$$\begin{aligned} \Delta u_i &= f(t_i + \Delta t_i) - f(t_i), \\ &\approx \Delta t_i f'(t_i), \\ &\approx \Delta s_i M f'(t_i). \end{aligned} \quad (8)$$

Let J_i denote $f'(t_i)$, a 3×3 Jacobian, which equals

$$J_i = \frac{1}{3} \begin{bmatrix} X_n^{-1/3} X_i^{-2/3} & 0 & 0 \\ 0 & Y_n^{-1/3} Y_i^{-2/3} & 0 \\ 0 & 0 & Z_n^{-1/3} Z_i^{-2/3} \end{bmatrix} \cdot \begin{bmatrix} 0 & 500 & 0 \\ 116 & -500 & 200 \\ 0 & 0 & -200 \end{bmatrix}. \quad (9)$$

Then the increase of ΔE due to the additive noise in the testing set can be calculated as

$$(\Delta E_i)^2 = \|\Delta u_i^t\|_2^2 = \Delta s_i A_i (\Delta s_i)^t, \quad (10)$$

where $A_i = M J_i J_i^t M^t$. The size of its entries is inversely proportional to the XYZ tristimulus values to the power of $4/3$. This implies that the effect of the noise is more serious with dark samples, or color samples with small X or Y or Z values. Consider a special case when the noises in the 3 channels are independent, identically distributed (i.i.d.) random variables with zero mean and variance σ^2 . Then

$$\begin{aligned} \mathcal{E}[(\Delta E_i)^2] &\leq \mathcal{E}[(\Delta E_i)^2] = \mathcal{E}[\Delta s_i A_i (\Delta s_i)^t], \\ &= \sigma^2 \cdot \text{tr}[A_i], \end{aligned} \quad (11)$$

where $tr[\cdot]$ denote the trace of the matrix. Thus, in this case,

$$\mathcal{E}[\Delta E_i] \leq \sigma \cdot \sqrt{tr[A_i]}. \quad (12)$$

Next, in order to investigate the effect of measurement error in the training set on the model performance, let us assume that ΔS_1 is the stack of the camera measurement errors for the training set. Let M be the calibration model identified from noise-free camera measurements; and let M' be the model identified from noisy camera measurements. That is,

$$M = S_1^\dagger T_1 \quad \text{and} \quad M' = (S_1 + \Delta S_1)^\dagger T_1.$$

Let t_j be the tristimulus row vector of the j th test sample. Then the tristimulus variation Δt_j due to this model variation is

$$\Delta t_j = s_j M' - s_j M = s_j ((S_1 + \Delta S_1)^\dagger - S_1^\dagger) T_1. \quad (13)$$

Similar to the previous analysis, using a first order approximation, the variation of the tristimulus row vector in the $L^*a^*b^*$ color space is

$$\Delta u_j \approx \Delta t_j J_j = s_j ((S_1 + \Delta S_1)^\dagger - S_1^\dagger) T_1 J_j. \quad (14)$$

Hence the increase of ΔE for the j th test sample resulting from the additive noise in the training set, can be calculated by

$$\Delta E_j = \|\Delta u_j^t\|_2 = \|J_j^t T_1^t ((S_1 + \Delta S_1)^\dagger - S_1^\dagger)^t s_j^t\|_2. \quad (15)$$

Using inequalities for the p -norm and Frobenius-norm,²⁷ ΔE_j can be upper bounded by

$$\begin{aligned} \Delta E_j &\leq \|J_j^t T_1^t\|_2 \cdot \|((S_1 + \Delta S_1)^\dagger - S_1^\dagger)^t\|_2 \cdot \|s_j^t\|_2, \\ &\leq \|J_j^t T_1^t\|_2 \cdot \|((S_1 + \Delta S_1)^\dagger - S_1^\dagger)^t\|_F \cdot \|s_j^t\|_2, \\ &\leq \|J_j^t T_1^t\|_2 \cdot \|s_j^t\|_2 \cdot 2 \|\Delta S_1\|_F \cdot \\ &\quad \max\{\|S_1^\dagger\|_2^2, \|(S_1 + \Delta S_1)^\dagger\|_2^2\}, \\ &= K_j \cdot \max\{\|S_1^\dagger\|_2^2, \|(S_1 + \Delta S_1)^\dagger\|_2^2\} \\ &\quad \cdot \|\Delta S_1\|_F, \end{aligned} \quad (16)$$

where $K_j = 2 \cdot \|J_j^t T_1^t\|_2 \cdot \|s_j^t\|_2$. Let us assume that $\text{rank}(S_1) = \text{rank}(S_1 + \Delta S_1)$ and $\|\Delta S_1\|_2$ is small, then²⁸

$$\|(S_1 + \Delta S_1)^\dagger\|_2 \approx \|S_1^\dagger\|_2,$$

which implies that

$$\max\{\|S_1^\dagger\|_2^2, \|(S_1 + \Delta S_1)^\dagger\|_2^2\} \approx \|S_1^\dagger\|_2^2.$$

The above assumptions are very reasonable since (i) both S_1 and $S_1 + \Delta S_1$ have rank 3 unless the training set is a 2-D or even 1-D color set, (ii) $\|\Delta S_1\|_2$ is usually small

unless the device has very low SNR. Under these assumptions ΔE_j is upper-bounded by

$$\Delta E_j \leq K_j \cdot \|S_1^\dagger\|_2^2 \cdot \|\Delta S_1\|_F. \quad (17)$$

If we again assume that the camera measurement noise is i.i.d. with zero mean and variance σ^2 , then

$$\begin{aligned} \mathcal{E}[\|\Delta S_1\|_F^2] &= \mathcal{E}\left[\sum_{k=1}^{N_1} \sum_{l=1}^3 ((\Delta S_1)_{(k,l)})^2\right], \\ &= \sum_{k=1}^{N_1} \sum_{l=1}^3 \mathcal{E}[(\Delta S_1)_{(k,l)}^2], \\ &= 3N_1 \sigma^2. \end{aligned} \quad (18)$$

That is,

$$(\mathcal{E}[\Delta E_i])^2 \leq \mathcal{E}[(\Delta E_j)^2] \leq K_j^2 \cdot \|S_1^\dagger\|_2^4 \cdot 3N_1 \sigma^2. \quad (19)$$

Hence

$$\mathcal{E}[\Delta E_i] \leq K_j \cdot \|S_1^\dagger\|_2^2 \cdot \sqrt{3N_1} \sigma. \quad (20)$$

Color calibration results

Due to the linearity of the CCD array and the access to raw rgb data from our camera, gray balance is unnecessary when the range of operation is between 0 and 0.7 on a 0-1 scale using a fixed exposure time. The calibration results were quantified in term of ΔE units in $L^*a^*b^*$ color space. The reference white points were set by combining the highest measured Y value from each data set with the chromaticity $(x, y) = (0.3127, 0.3291)$ for D65.

In our first calibration test, a set of 180 color samples were created and displayed on a CRT monitor. Within this data set, a total of 51 color samples which consisted of pure red, green, and blue patches were used to find the calibration model \widehat{M}_{CRT} . This model was then used on the training set itself to see how well this calibration model works. We also used this model to estimate the tristimulus values of the remaining 129 color samples. The ΔE 's between model prediction and measurement for both cases were calculated; and the histograms are shown in Fig. 4.

We applied the same calibration procedure to a Bio-form shade guide. Due to the limited size of this data set, we evaluated the model performance in a statistical sense. The calibration procedure was conducted 100 times. In each trial, seventy-five percent of the shades were randomly chosen as the training set and the rest as the testing set. The average ΔE 's for both the training set and the testing set were recorded in each trial. The calibration experiment for 11 extracted human teeth was conducted in the same fashion. In Table I, we summarize the characteristics of the calibration samples and the model performance for our calibration experiments.

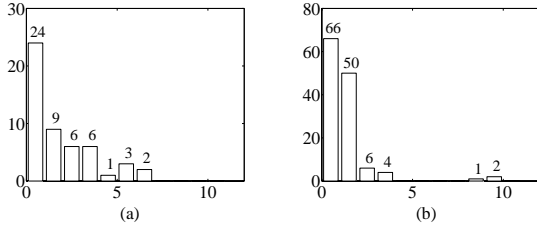


Figure 4: Calibration result for 180 CRT color samples: (a) the ΔE histogram of the 51 training samples. Its average is 1.8159. (b) the ΔE histogram of the 129 test samples. Its average is 1.3064. The average ΔE over the entire 180 CRT color samples is 1.4507.

Data set	Overall ΔE	Principal component analysis (one,two,three) bases	Color space
CRT	1.4507	(61.74%, 80.92%, 99.65%)	3-D
Shade	0.9703	(94.53%, 98.24%, 99.01%)	2-D
Teeth	1.5745	(91.73%, 97.91%, 99.29%)	2-D

Table I. 3-D calibration model: the data set characteristics and the model performance. The accumulated percentages of the energy in the spectral power distribution characterized by the first one, the first two, and the first three basis functions from a principal component analysis are computed; and they are used to classify the dimension of the color space. Here we use 97% as the threshold.

Finally, we wish to determine the number of bits required for our test samples so that quantization of these samples does not degrade the performance of the model by more than a specified amount. We will use $1\Delta E$ unit here. This can be done by averaging the upper bound given in Eq. (12) over the N_2 test samples. Let Φ denote this average. Then

$$\Phi = \frac{1}{N_2} \sum_{i=1}^{N_2} \sigma \cdot \sqrt{\text{tr}[A_i]} = \sigma \cdot \bar{A}, \quad (21)$$

where, $\bar{A} = \frac{1}{N_2} \sum_{i=1}^{N_2} \sqrt{\text{tr}[A_i]}$. Assuming that the quantization step size is Δ , then the standard deviation σ in Eq. (12) is given by $\Delta/(\sqrt{12})$. Setting $\Phi = 1$ and solving for Δ , we obtain

$$\Delta = \sqrt{12}/\bar{A}. \quad (22)$$

Since the signal is normalized to a 0-1 scale, the number of bits b_{test} required to achieve an average upper bound of one ΔE unit is given by

$$b_{\text{test}} = -\log_2 \Delta. \quad (23)$$

A similar analysis can be done on the effect of quantization in the training set by averaging the upper bound given in Eq. (20) over the testing set. Let Υ denote this average. Then

$$\Upsilon = \bar{K} \|S_1^\dagger\|_2^2 \cdot \sqrt{3N_1} \cdot \Delta/(\sqrt{12}), \quad (24)$$

where

$$\bar{K} = \frac{1}{N_2} \sum_{i=1}^{N_2} 2 \cdot \|J_i^t T_1^t\|_2 \cdot \|s_i^t\|_2. \quad (25)$$

Setting $\Upsilon = 1$ and solving for Δ , we obtain

$$\Delta = \frac{2}{\sqrt{N_1} \cdot \bar{K} \cdot \|S_1^\dagger\|_2^2}. \quad (26)$$

The number of bits b_{training} required to achieve an average upper bound of one ΔE unit is again given by Eq. (23).

We applied these analyses to our calibration samples; and the results are tabulated in Table II. With our 12-bit camera data, we see that test sample quantization is not a limiting factor for our calibration samples. For quantization of the training samples however, our bound appears to be quite loose.

Data	b_{test}	b_{training}
CRT	10 bits	15 bits
Shade	9 bits	25 bits
Teeth	10 bits	24 bits

Table II. Estimation of the number of bits required to limit the effect of quantization to an increase in error of one ΔE unit. We consider separately the effect of quantizing the test samples and the training samples.

To confirm this suspicion, we simulated the effect of quantization in the testing set (Simulation I) and in the training set (Simulation II) by adding uniformly distributed random noise to the camera measurements. The results are tabulated in Table III. Note that the ΔE between the estimated tristimulus vector for the noisy color sample and the estimated tristimulus vector for the noise-free color sample is averaged over 100 trials, then averaged over all the test samples. The simulation results show that the upper bounds for Simulation I are tight; and those for Simulation II are very loose. In fact, from the ratio γ , we see that Υ overestimates the b_{training} by about 7, 17, and 14 bits, respectively.

Data set	Sim. I ΔE	Bound Φ	Sim. II ΔE	Bound Υ	ratio (γ) (bits)
CRT	0.1575	0.1792	0.0308	4.5784	7
Shade	0.0792	0.0877	0.0567	5119.7	17
Teeth	0.1558	0.1795	0.1397	3055.8	14

Table III. Simulation results of the average increase of ΔE over the testing set in 100 trials. Simulation I investigates the effect of measurement error in the testing set on the model performance; and its average upper bound is calculated from Eq. (21). Simulation II investigates the effect of measurement error in the training set on the model performance; and its average upper bound is calculated from Eq. (24). Here, $\gamma = -\log_2((\Delta E \text{ in Sim. II})/\Upsilon)$ bits.

The reason that the upper bounds of Simulation II are especially loose for both the Bioform shade guide and the extracted human teeth is that they are actually 2-D color sets, which violates the assumption in the error analysis section.

Discussion and conclusion

There are several sources which would result in the calibration errors, such as the error from the XYZ measurements, the error from the 3-D model assumption, or the error due to quantization in the camera measurements. Our simulation shows that our 12-bit precision camera is adequate to ensure that the average ΔE contributed by the quantization process is less than one.

The calibration model we proposed is simple; and it performs well for our 3-D color sets. Based on a just noticeable difference of $2.3\Delta E$ units,²⁹ the performance of our model for the extracted human teeth is adequate. However, we would like to obtain even more accurate results. One factor that currently limits the performance of the model is the significant amount of highlight on the tooth samples. This tends to result in a measurement of the color of the illuminant rather than that of the tooth. This is a major source of error in our calibration procedure. We are investigating the possibility of integrating a polarizer into our system to reduce the highlight component, and thus improve the calibration precision.

References

1. J.M. Leon, Shade Selection - The Art and Science of Color Matching, *Quintessence International*, Vol. **8**, pp. 851-859, 1982.
2. J.D. Preston, Current Status of Shade Selection and Color Matching, *Quintessence International*, Vol. **1**, pp. 47-58, 1985.
3. T.P. van der Burgt, J.J. ten Bosch, P.C.F. Borsboom and A.J.M. Plasschaert, A New Method for Matching Tooth Colors with Color Standards, *Journal of Dental Research*, Vol. **64** No. **5**, pp. 837-841, 1985.
4. N.R. Hall, Tooth Colour Selection: the Application of Colour Science to Dental Colour Matching, *Australian Prosthodontic Journal*, Vol. **5**, pp. 41-46, 1991.
5. R.C. Sproull, Color Matching in Dentistry. Part II: Practical Applications for the Organization of Color, *The Journal of Prosthetic Dentistry*, Vol. **29**, pp. 556-566, 1973.
6. W.B. Schwabacher and R.J. Goodkind, Three-dimensional Color Coordinates of Natural Teeth Compared with Three Shade Guides *The Journal of Prosthetic Dentistry*, Vol. **64**, pp. 425-431, 1990.
7. L.L. Miller, Organizing Color in Dentistry, *Journal of the American Dental Association*, Special Issue No: **26E-40E**, 1987.
8. L.L. Miller, A Scientific Approach to Shade Matching. In Preston JD, ed. Perspectives in dental ceramics, *Proceedings of the Fourth Int. Symposium on Ceramics. Carol Stream, IL: Quintessence*, pp. 193-208, 1988.
9. W.J. O'Brien, C.L. Groh and K.M. Boenke, A One dimensional Color Order System for Dental Shade Guides, *Dental Materials*, pp. 371-374, 1989.
10. M. Macentee and R. Lakowski, Instrumental Colour Measurement of Vital and Extracted Human Teeth, *Journal of Oral Rehabilitation*, Vol. **8**, pp. 203-208, 1981.
11. T.W. Lund, W.B. Schwabacher and R.J. Goodkind, Spectrophotometric Study of the Relationship between Body Porcelain Color and Applied Metallic Oxide Pigments, *The Journal of Prosthetic Dentistry*, Vol. **53**, pp. 790-796, 1985.
12. T.P. van der Burgt, J.J. ten Bosch, P.C.F. Borsboom and W.J.P.M. Kortsmit, A Comparison of New and Conventional Methods for Quantification of Tooth Color, *The Journal of Prosthetic Dentistry*, Vol. **63**, pp. 155-162, 1990.
13. D. Ferreira and L. Monard, Measurement of spectral reflectance and colorimetric properties of Vita shade guides, *Journal of the Dental Association of South Africa*, Vol. **46**, pp. 63-65, 1991.
14. B.A. Wandell and J.E. Farrell, Water into Wine: Converting Scanner RGB to Tristimulus XYZ, *SPIE*, Vol. **1909**, pp 92-101, 1993.
15. B.A. Wandell and J.E. Farrell, Scanner Linearity, *Journal of Electronic Imaging*, Vol. **2**, pp 225-229, 1993.
16. G.D. Finlayson and M.S. Drew, The Maximum Ignorance Assumption with Positivity, *The Fourth Color Imaging Conference: Color Science, Systems and Applications*, pp 202-205, 1996.
17. J. Farrell, D. Sherman and B. Wandell, How to Turn your Scanner into a Colorimeter, *IS&T's Tenth International Congress on Advances in Non-impact Printing Technologies*, pp 579-581, 1994.
18. H.R. Kang, Color Scanner Calibration, *Journal of Imaging Science and Technology*, Vol. **36**, pp 162-170, 1992.
19. H.R. Kang, Color Scanner Calibration of Reflected Samples, *SPIE: Color Hard Copy and Graphic Arts*, Vol. **1670**, pp 468-477, 1992.
20. U. Lenz, Dr. Habil and R. Lenz, Digital Camera Color Calibration and Characterisation, *The Fourth IS&T/SID Color Imaging Conference: Color Science, Systems and Applications*, pp 23-24, 1996.
21. H. Haneishi, T. Hirao, A. Shimazu and Y. Miyake, Colorimetric Precision in Scanner Calibration Using Matrices, *Proceedings of the IS&T/SID 1995 Color Imaging Conference: Color Science, Systems and Applications*, pp 106-108, 1995.
22. H.R. Kang and P.G. Anderson, Neural Network Applications to the Color Scanner and Printer Calibrations, *Journal of Electronic Imaging*, Vol. **1**, pp 125-135, 1992.
23. D. Sherman and J.E. Farrell, When to Use Linear Models for Color Calibration, *IS&T/SID's 2nd Color Imaging Conference: Color Science, Systems and Applications*, pp 33-36, 1994.
24. Dentsply/York Division, Bioform Color Ordered Shade Guide, *Dentsply International Inc., York, PA 17405-0872*.
25. Kodak digital science, Programmer's Reference Manual for Models: DCS 420m, DCS 420c, DCS460m, DCS460c, DCS465m, DCS465c, NC2000, EOS-DCS 3, EOS-DCS 5, *Eastman Kodak Company, Rochester, NY 14650*.
26. P.L. Vora, J.E. Farrell, J.D. Tietz and D.H. Brainard, Linear Models for Digital Cameras, *IS&T's 50th Annual Conference*, pp 377-382, 1995.
27. G.H. Golub and C.F. Van Loan, Matrix Computations, *The Johns Hopkins University Press*, 1983.
28. P.A. Wedin, Perturbation Theory for Pseudo-inverses, *BITs*, Vol. **13**, pp 217-232, 1973.
29. M. Mahy, L.V. Eyckden, and A. Oosterlinck, Evaluation of Uniform Color Spaces Developed After the Adoption of CIELAB and CIELUV, *Color Res. Appl.*, Vol. **19** No. **2**, pp 105-121, 1994.